

Nanostructures in gas suspension

K. Siegmann and H.C. Siegmann

Swiss Federal Institute of Technology, Zurich, Switzerland

Recibido el 30 de octubre de 1998; aceptado el 12 de noviembre de 1998

Nanostructures in gas suspension grow by clustering of atoms and radicals, by surface condensation, and by agglomeration. We show that photoelectron spectroscopy may be performed on nanostructures in their natural gaseous environment, that is, without application of a vacuum or precipitation onto a substrate. Moreover, the photoelectric yield induced by pulsed lasers delivers a fingerprint of the bulk and surface properties and their dynamics. The most important application is to the nanostructures formed in combustion of fossil fuels found abundantly in the air in which we live. These nanostructures are important to the physics and chemistry of the atmosphere and furthermore act as vehicles transporting a number of dangerous compounds deep into the human respiratory tract. We show how such particles may be identified according to their source and measured with portable sensors. We also present data taken in several large cities around the globe and quantify the impact on human health.

Keywords: Nanostructures and human health

Las nanoestructuras en suspensión gaseosa crecen por acumulación de átomos y radicales, por condensación de superficies y por aglomeración, esto es, sin la aplicación de un cierto vacío o bien por precipitación sobre un sustrato. Más aún, la corriente fotoeléctrica inducida por pulsos de rayo laser suministra una característica de huella digital de las propiedades de volumen y de superficie y de su dinámica. La aplicación más importante se tiene en las nanopartículas provenientes de la combustión de hidrocarburos de fósiles, que se encuentran abundantemente en el aire en el cual vivimos. Estas nanoestructuras son importantes para la física y la química de la atmósfera y además actúan como un vehículo de transporte de un cierto número de compuestos peligrosos hacia las regiones profundas del aparato respiratorio. Mostramos cómo tales partículas pueden identificarse según su origen y cuantificarse mediante sensores portátiles. Presentamos igualmente muestreos tomados en varias metrópolis alrededor de nuestro globo terrestre, cuantificando su impacto en la salud humana.

Descriptores: Nanoestructuras y salud humana

PACS: 94.10.Fa

1. Introduction

Particles suspended in gases may be divided into microparticles and nanoparticles. Microparticles are visible because they scatter the light with great efficiency, they impact on obstacles around which the gas carrying them is following, and they may be removed in electrofilters. However, the nanoparticles are hardly visible because they scatter the light only very weakly, and they follow the stream lines of the carrier gas, hence do not impact on obstacles at atmospheric gas pressure. Their removal must rely on diffusion to surfaces, hence a particle filter has to be constructed very differently, unfortunately, the inner part of our respiratory system, in particular the alveoles of the lung, are a quite effective filter for the nanoparticles. The lungs of the stone age hunter found in the ice of the alpine glaciers is loaded with nanoparticles giving a vivid picture of this lifestyle and his exposure to nanoparticles from combustion of organic matter [1]. Today, the evidence is increasing that nanoparticles suspended in ambient air are toxic and have a severe impact on public health, shortening the life expectancy even in allegedly clean cities such as the city of Zurich by as much as several years [2, 3].

A new thinking must be developed to quantify the nanoparticles and to detect their physical and chemical prop-

erties. This arises because nanoparticles resist definition in terms of traditional metrological properties such as mass, volume and diameter. Nanoparticles in gas suspension often exhibit bizarre shapes formed by random or interaction assisted agglomeration of much smaller primary solid particles. The agglomerates possess holes as well as internal and external surfaces that are much larger than commonly imagined. A surrogate concept for defining a size of such an object is the "mobility diameter". This "diameter" is defined as the diameter of a sphere with one single elementary charge having the same electrical mobility as the agglomerate. Many individual shapes and densities are summarized under one specific mobility diameter. However, when such nanoparticles contain liquid matter or when water condenses on them, the surface tension of the liquid tends to contract the structure to a spherical particle with little hollows inside. This is how nanoparticles may change size, shape, and density when released into the atmosphere, or when transported into the moist respiratory tract. Whether or not water condenses on the nanoparticles depends on the chemical properties of the surface: if it is hydrophobic like in the case of the primary particles from diesel motors, water will hardly condense [4]. For the impact on the living organism, the surface properties are essential. Hydrophobic substances that dissolve in the fatty tissue like the polycyclic aromatic hydrocarbons (PAH) are most

difficult for the body to dispose off and may induce cancer in humans [5]. Hence, instead of trying to determine all the thousands of chemicals that are present for instance in the ubiquitous nanoparticles from combustion, one must try to focus on the surface properties and distinguish first of all hydrophilic from hydrophobic substances. In this paper, we will show that rather simple physical methods exist to reasonably quantify such basic properties of nanoparticles.

With respect to impact on health, it is mandatory to distinguish particles from different sources such as windblown dust, wear and tear of tires, or harmless salt particles generated by the surf of the ocean, from the dangerous particles in diesel fumes and cigarette smoke. Each of these particles carries a different blend of chemicals and therefore poses a different health risk. We will describe two physical principles of putting electrical charges on particles and show how this electrical charging may be used to characterize basic properties of nanoparticles and even determine the sources from which the particles have been emitted.

2. Measurement of physical and chemical properties

2.1. Diffusion charging (DC)

If the gas carrying the particles contains positive or negative ions, these ions have the tendency to attach to the particles by diffusion and thus charge the particles electrically. Positively charged ions for instance can be produced by a glow discharge forming in the neighborhood of a very thin wire. The positive ions are repelled from the wire which is at positive potential and migrate through the space containing the particles to the outer negative electrode. In this migration, there is a probability that they attach to the particles. If this happens, the particle carries the charge away. Further downstream, the gas containing the particles passes through a filter in which all particles are precipitated. The electric current i_{DC} flowing from the filter to ground potential is measured and tells us how many positive ions produced in the glow discharge have attached themselves to particles. We have

$$\frac{i_{DC}}{i_0} = \text{Const} \cdot \eta(R) \cdot Z(R) \cong \text{const} \cdot R^2 \cdot Z(R), \quad (1)$$

where i_0 is the electric current in the glow discharge, $\eta(R)$ the attachment coefficient of positive ions to neutral particles and $Z(R)$ the density of particles. For particles of $R \leq 100$ nm, $\eta(R) \cong R^2\pi$, that is the attachment is proportional to the cross section of the particles. This arises because the mean free path of the ions in the carrier gas is larger than the particle diameter for particles below 100 nm diameter. In that case, the ions move on trajectories like in vacuum, and the probability to hit the particle is simply given by its cross section. Hence with particles below 100 nm, an instrument based on diffusion charging will measure the total surface of the particles without being sensitive to the chemistry, as an ion sticks to any surfaces once it hits it. It is customary to call

the surface equivalent determined by diffusion charging the "Fuchs surface". It comprises the outer surface of agglomerates only that can be reached by diffusion.

2.2. Photoelectric charging (PC)

If the gas carrying the particles is irradiated with ultraviolet light of energy $h\nu$ below the threshold for ionisation of the gas molecules but above the photoelectric threshold Φ of the particles, photoelectrons may be emitted from the particles. The photoelectrons thermalize in the carrier gas, and if it contains oxygen, they will attach to the oxygen molecules and form a negative ion. The negative ion will diffuse back to the particle if it is about 1 micrometer or larger in size. However, for particles smaller than the mean free path of the negative ion, backdiffusion becomes improbable and the particle remains with a positive charge while the negative ion or the photoelectron diffuses to the walls. It is also possible to remove the negative ions by an alternating electric field which does not affect the positively charged particles because their electrical mobility is small [6]. The current produced by the photoelectric emission from the particles is now again measured by precipitating all particles in a filter and measuring the current i_{PC} flowing from the filter to ground potential. i_{PC} is related to the optical absorption α of the ultraviolet light and the probability Y with which the electronic excitation produces an electron that can escape the surface barrier potentials:

$$\frac{i_{DC}}{i_{h\nu}} = \text{Const} \cdot \alpha \cdot Y \cdot R^2 \pi \cdot Z(R), \quad (2)$$

$i_{h\nu}$ is the current of photons produced by the KrBr excimer lamp with $h\nu = 6.0$ eV ($\lambda = 207$ nm). We see that the signal from the photoelectric instrument is also proportional to the outer surface of the particles, but it contains factors that depend on the bulk and surface chemical properties, namely α and Y respectively. It turns out that particles in the nanometer range are extremely efficient photoemitters. Furthermore, their photoelectric yield Y is governed by adsorbates to a much larger degree than is observed with flat macroscopic surfaces [7]. While these phenomena have not yet found a satisfactory theoretical explanation, they are very useful to obtain in situ information on the chemical composition of the particle and its surface. Of particular importance are the polycyclic aromatic hydrocarbons (PAH). If these flat and large molecules are adsorbed on the particle surface, the photoelectric yield Y increases dramatically by an order of magnitude at coverages below one monolayer. At ambient temperatures, the PAH with less than 4 benzene rings are not adsorbed at the surface, but the PAH with 4 and more rings are, and hence can be detected with great efficiency. It turns out that the photoelectric current is in fact proportional to the total mass of particle adsorbed PAH (PPAH) quite independently of the chemical nature of the particles [8]. This amazing phenomenon can presumably be explained by the large

absorption cross section of the π -electrons in the PAH's together with the enhanced density of states near the vacuum level. The general picture explaining the large enhancement of the photoelectric yield by adsorption of PAH is that the PAH act as photonic antennas concentrating the energy of the absorbed photon near the surface.

It turns out that the signal generated by PC is also proportional to the reading from instruments such as the aethalometer detecting the amount of "black" carbon contained in nanoparticles that are previously precipitated on a filter. This follows from Eq. (2) where PC is proportional to the optical absorption α besides the photoelectric yield Y .

The most important feature of PC is however that it is zero when the surface of the particles consists of water. Hence one readily can distinguish between the dry or hydrophobic and the wet or hydrophilic particles. Furthermore, PC is only effective for nanoparticles as it does not occur with microparticles. This makes it ideally suited to selectively detect the respiratory particles, that is the particles that are precipitated in the inner respiratory system.

Photoelectric charging is a unique tool to study fundamental properties of nanoparticles and their surfaces in gas suspension without precipitating the particles onto a substrate. So far, the following applications have been found:

1. Material and surface specific detection of nanoparticles in ambient air. This will be shown below on the example of the particles generated in combustion.
2. Detecting the process of heterogeneous catalysis on the surface of the nanoparticles. As an example, we have studied soot reduction by fuel additives [9].
3. Measuring the dynamics of molecular adsorption at the particle surface. In this application, the light pulses of a duration of nanoseconds from a laser have to be used for PC [10].
4. Measuring the dynamics of the electrons within the nanoparticle. For this, one needs a pump and a proper light pulse of a duration in the range of femtoseconds. The pump pulse optically excites the electrons within the particle, and the delayed probe pulse detects those electrons that are still excited by photoemitting them into the carrier gas [11].
5. Chiral nanoparticles: Particles that are built from chiral molecules such as aminoacids will absorb left and right circularly polarized light with somewhat different probability. This selectively detects nanoparticles of biological origin [12].

We now proceed to some simple experiments with particles generated in various types of combustion.

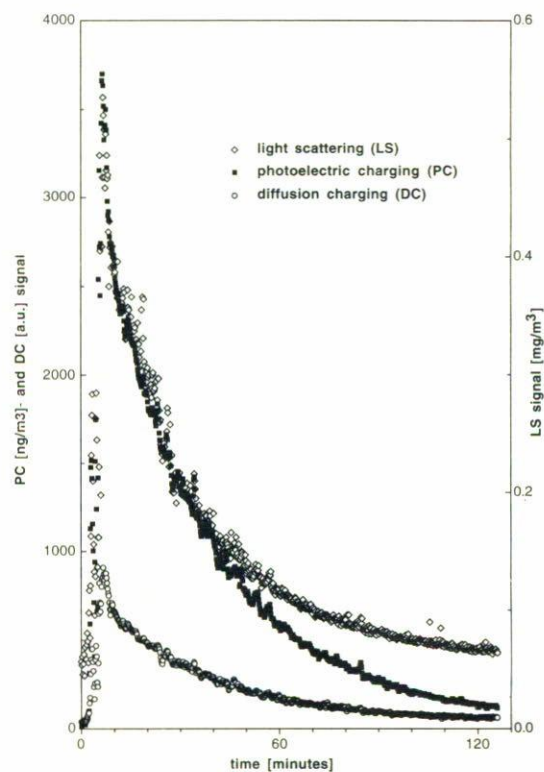


FIGURE 1. Aerosol from a sooting candle flame in a closed room (The room is filled with aerosol, then the candle is blown out). The signals PC and DC are shown as they decay with time. Light scattering (LS) at 90° of the light from a GaAs-diode is also shown. The calibration of the LS signal does not apply, it is valid for Arizona dust.

3. Model experiments

Simple experiments demonstrate how the simultaneous application of diffusion charging and photoelectric charging allows one to distinguish the particles from various sources as desired. Fig. 1 shows a model experiment with soot particles from a paraffin candle. If the candle burns correctly, it does not emit any soot particles. However, if the flame is cooled by putting a metal spoon into it, one sees a thin filament of soot rising with the hot gases. $\bar{1}$ min of soot production is enough to fill a room of 50 m^3 with very fine soot particles, after allowing a few minutes for homogeneous distribution, see Fig. 1. These soot particles have PAH adsorbed on their surface, hence are extremely efficient photoemitters. It should be noted that PAH are formed in any incomplete combustion of organic material, but the amount of PAH varies widely depending on the fuel and the conditions of the combustion. Hence PAH can be used as a label of combustion generated particles and their density at the particles surface will be characteristic for each type of combustion.

Figure 1 shows that the signal from the 2 instruments located in the room decreases with time, but the rate at which the signal decreases is different in each case. According to

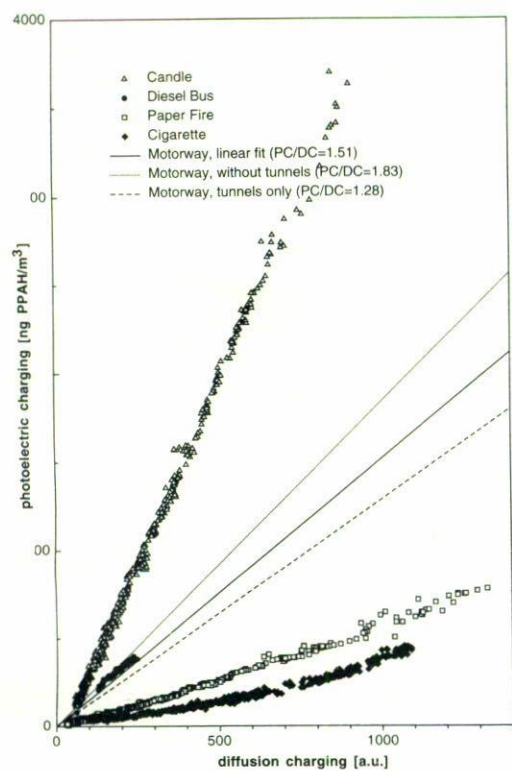


FIGURE 2. Photoelectric charging (PC) against diffusion charging (DC) for different combustion aerosols. The slope of the curves is characteristic for the aerosol source. Linear fits for aerosols found on motorways are also shown. They mainly consist of diesel emissions. The data points are for diesel particles collected in a plastic bag at the bus stop.

Eqs. (1) and (2), the ratio of diffusion charging i_{DC} and photoelectric charging i_{PC} is given by

$$\frac{i_{PC}}{i_{DC}} = \text{const} \cdot \alpha Y. \quad (3)$$

Hence it should not change provided that neither the bulk nor the surface chemistry of the particles changes. Figure 2 shows that this is indeed the case as i_{PC} plotted against i_{DC} yields a straight line with candle soot. Figure 2 also shows results of experiments done in the same way but with different types of combustions. We see that burning a sheet of paper produces particles with constant chemistry as well, but the slope is very different compared to candle soot, hence the particles produced in combustion of paper are chemically different and can thus easily be distinguished from the particles produced in a paraffin candle.

Figure 2 also shows results with particles produced by smoking a cigarette in the room. In that case, i_{PC} vs. i_{DC} does not produce a straight line. This indicates that the particles of cigarette smoke change their surface chemistry with time whereby the efficiency of photoelectric charging is reduced. Note that the older particles are at lower currents in Fig. 2. It is known that nanoparticles in cigarette smoke contain liquid material, therefore the observed reduction in PC

per unit surface area may also indicate a change in particle shape.

Also plotted are the yield curves of photoelectric charging particles found on the motorway close to Zürich. Particles in the street tunnels seem to exhibit lower photoelectric yield compared to particles on the open motorway. Generally, the yield of motorway particles is much higher compared to the yield of cigarette smoke.

We will present evidence below that the lower photoelectric yield per unit surface area observed in street tunnels is due to the formation of new hygroscopic particles in gas to particle reactions probably involving SO_x and NO_x emissions from the motor vehicles. The model experiment shows that the specific photoelectric yield, that is, the yield per unit surface area stays constant with candle and paper fire particles (in the absence of solar irradiation) while it decreases with cigarette particles. It is also clear that the particles from different combustion sources are readily distinguished by their different specific photoelectric yield. We note that the particles are removed from the room by ventilation through holes in the door, windows and cable ducts, by diffusion to the walls and furniture, and by agglomeration and subsequent sedimentation. The particle loss by ventilation is however dominant. It is in fact possible to determine the air exchange of a room or a building with the outside world by measuring the loss of particles created inside or the gain of particles from outside stemming for instance from vehicle traffic [13].

The most important result from the model experiments is that Diesel particles found on the motorway can easily be recognized by their high photoelectric yield compared to cigarette smoke. In practice, the distinction between Diesel and cigarette smoke is important as most of the personal exposure comes from these sources. Hence the simultaneous application of PC and DC makes possible the source attribution of combustion aerosols.

It should be noted that, at least in air as a carrier gas, particles from other than combustion sources can generally not be charged photoelectrically because of the absence of PAH. Hence such particles will produce a signal only in optical scattering of light and in diffusion charging. There are exceptions from this rule: namely fresh metal particles produced for instance in welding [14], and CuCl-particles produced in outgassing of volcanic magma [15] are also efficient photoemitters. However, these particles lose their photoelectric activity in ambient air in a few minutes by oxidation. In the regular urban environment it is safe to assume that particles which can be charged photoelectrically by light with energy $h\nu = 6.0 \text{ eV}$ are generated in combustion of organic material. The PAH's are unique in that they can resist oxidation in ambient air for a long time at least in the absence of ozone and/or ultraviolet light. The photoelectric charging is also suitable to detect the degradation of PPAH in the atmosphere, but this does not have to be considered in close proximity to measurements close to the source, that is to streets or motorways.

4. Field measurements

We have built battery operated portable instruments for detection of the particles based on PC and DC. The data are automatically recorded and can be extracted later. It turned out that it is useful to also have independent information on PM-10, that is the mass of particles with larger diameter up to 10 μm . For this purpose, we used a portable, battery operated instrument based on the scattering of infrared light from a GaAs-laser-diode (LS). This instrument is commercially available. It has an impactor at the entrance which removes all particles with an inertia diameter of more than 10 μm . The LS-instrument is calibrated in mass per m^3 . However, the calibration is for "Arizona dust" which exhibits a wide size distribution. We have recalibrated this instrument for the particles found on motorways. This is possible because the PC-instrument is calibrated in mass of particles bound PAH per m^3 , and because independent chemical analysis of filter extracts from motorway samples shows that 0.8% of the motorway particle mass consists of PAH [16]. It turns out that the readings of the LS-instrument calibrated with Arizona dust have to be multiplied with 0.3 to correctly account for the total mass PM-10 of particles below 10 μm found on motorways.

The three instruments were carried in a Rucksack or put on the dashboard in a car. Whenever possible, the windows of the car were opened. The air was sampled from one point located close to the height at which people breathe. Exhaustive long term studies have been performed in a road tunnel near Zürich, Switzerland, known as the Gubrist tunnel. This tunnel is divided into two separate tubes which each have one way traffic only. The speed limit is 100 km/h, and the tunnel is 3.250 km long. Hence it takes at least 2 min to pass the tunnel. Measurements were recorded every 10 sec. There is no ventilation in the tunnel, except for the wind produced by the movement of the vehicles. This wind averages to 9 m/sec resulting in a residence time of the air in the tunnel of 6 min. E. Weingartner *et al.* [16] have continuously measured the chemical and physical properties of the aerosol in that tunnel. Of particular interest is the size distribution and the chemical composition of the particles. At the entrance, the size distribution is broad, and there are maxima in the density of $Z(R)$ at $2R = 20$ nm and $2R = 100$ nm. At the exit, the size distribution is sharper and exhibits only one maximum at $2R = 120$ nm. We suspect the 20 nm particles are condensates forming in gas to particle reactions on cooling the exhaust.

Figure 3 shows the recording of the 3 instruments on a trip from ETH Zürich to Baden and back. Measurements were recorded every 10 sec. After about 9 min, the motorway is reached and after 10 min the entrance of the Gubrist tunnel.

A second short tunnel named Baregg is reached after 20 min. After this, the return is on the same motorway to pass Baregg and Gubrist in the opposite direction. There was heavier traffic on the way back.

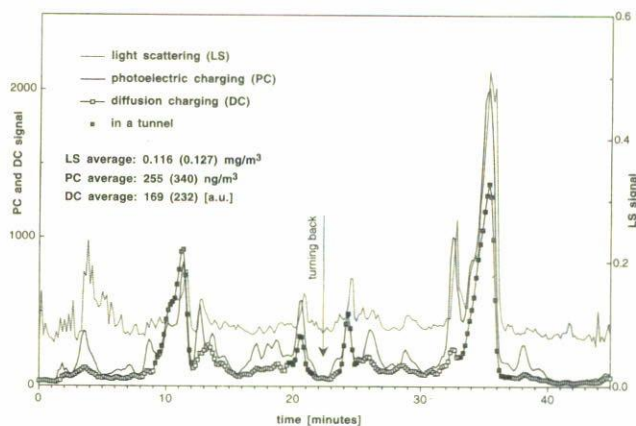


FIGURE 3. LS, PC and DC signals from a trip on the motorway from Zurich to Baden (Switzerland) and return (18.Nov.1997). The two tunnels are marked with filled squares. The calibration of LS is for Arizona dust. It has to be multiplied by 0.3 to correctly reproduce the mass of the motorway aerosol in relation to the total mass of particles bound PPAH as observed by PC.

Light scattering (LS) clearly shows a background signal that is independent of the tunnels, and even does not change when the motorway is left or entered. This must be due to particles from other sources than automotive traffic. The numbers given at the abscissa are with the factory calibration, but for the motorways one has to multiply these values with 0.3.

Photoelectric charging shows sharper structures. It is also obvious that the ratio PC/DC changes in the tunnels with DC gaining more strength. This is explained by the new particles generated in gas to particle reactions and agrees with the findings of E. Weingartner *et al.* [16].

With the specific calibration, the average ratio PC/LS = 0.73% on the whole trip. That is the average particle mass PM-10 was 34.8 $\mu\text{g}/\text{m}^3$ and the average PPAH-mass 255 ng/m^3 , hence about 0.73% of the particle mass consists of particle bound polycyclic aromatic hydrocarbons. Omitting the first 10 min, that is the readings on the access to the motorway, PM-10 = 38.1 $\mu\text{g}/\text{m}^3$, PPAH = 340 ng/m^3 , and PC/LS = 0.89%. This illustrates once more that there are other particles on the access road in addition to those produced by the vehicles. The other particles are not produced in combustion as they do not produced a signal in PC.

The ratio PC/DC = 1.51 in the average, that is the aerosol on the motorway is identified as particles from Diesel engines according to Fig. 2. This agrees with E. Weingartner *et al.* [16] who found that the aerosol in the Gubrist tunnel is dominated by Diesel vehicles.

Figure 4 shows PC and LS data on the way from the airport CDC to the center of Paris. Noteworthy is particularly a one way five tracked tunnel entered at 9.57 h and left at 10.13 h. Due to the regularly occurring traffic jam, there is no ventilation of this comparatively short tunnel. The growth of the particles in the tunnel as evidenced by the growth of LS is much more pronounced compared to the Gubrist-tunnel in Switzerland due to much higher exhaust concentrations. Note

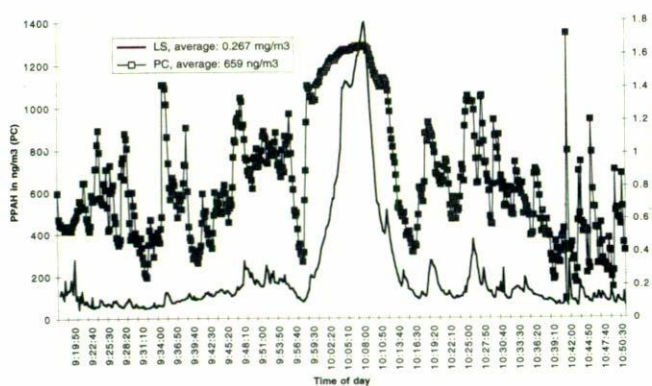


FIGURE 4. PC (squares) and LS (bold line) for trip on a motorway in Paris (Aéroport CDG to rue de Faubourg-Poissonniere, 8.Sept.1997). A tunnel is traversed from 9:57 to 10:13. Calibration of LS as in Fig. 3.

that LS is proportional to the sixth power of the particle diameter, hence it responds dramatically to the growth of the condensates in the tunnel. Note also that the particles detected by PC, that is the particles nucleated in the combustion zone, are not affected by condensation.

The average PM-10 was $80.1 \mu\text{g}/\text{m}^3$ using the calibration from the Gubrist tunnel in Switzerland, the average PPAH $659 \text{ ng}/\text{m}^3$. Hence $\text{PC}/\text{LS} = 0.82\%$, that is 0.82% of the particle mass are PAH.

The constantly higher PPAH-values everywhere in and around Paris are due to the fact that 40% of the passenger cars are Diesel driven while in Switzerland the percentage of Diesel passenger cars is 2% only. Hence the poorer air quality in the city of Paris compared to Zurich must be attributed to the tax laws favoring the use of Diesel vehicles.

Figure 5 shows PC and LS data from the first half of the highway from Tokyo to Nikko. There is no tunnel on this highway.

The average PM-10 was $111 \mu\text{g}/\text{m}^3$, using the calibration from Switzerland, the average PPAH $926 \text{ ng}/\text{m}^3$. Hence $\text{PC}/\text{LS} = 0.83\%$, which is identical to the value obtained on Swiss and French motorways within uncertainties, and identifies the sources of the particles as Diesel motors. It appears that more trucks are circulating on the motorways in Japan maybe due to JIT (just in time delivery). This then would explain why the particle loading of the air on motorways is even higher than in France.

The fact that the PC/LS ratios in the industrialized countries are identical within uncertainties is surprising. Note that the constancy of this factor is independent of any absolute calibration of the instruments. Due to differences in the vehicles, fuel and particularly the weather conditions one might have expected significant differences especially in the surface properties of the particles. The results presented here clearly demonstrate that this is not the case. It can be understood by the fact that motorways are source dominated, that is the influence of solar irradiation may be important with older par-

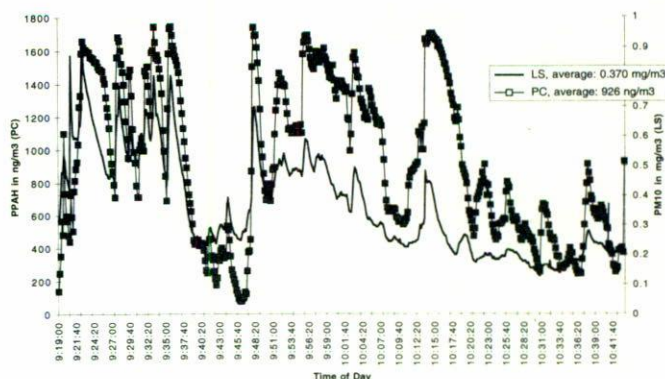


FIGURE 5. PC (squares) and LS (bold line) for a trip on a motorway in Tokyo (first part of the Highway Tokyo-Nikko). LS calibration as in Fig. 3.

ticles only. There is even no seasonal variation of the average PC/LS ratio. For instance, on a trip from Zurich to Basel in July 1997 we obtained $\text{PC}/\text{LS} = 0.82\%$, while the average PPAH was $134 \text{ ng}/\text{m}^3$ and PM-10: $16.3 \text{ mg}/\text{m}^3$ (the data on Fig. 3 were taken in November). However, the intensities of the aerosols vary quite dramatically. One then expects the same kind of health problems yet with different intensities from nanoparticles on motorways all over the globe.

5. Summary and impact on public health

The polycyclic aromatic hydrocarbons (PAH) are produced abundantly in any incomplete combustion of organic material. Due to the strainless arrangement of sp^2 -hybridized carbon atoms in six membered rings and, above all, the energy gain from the delocalized π -electrons, PAH are thermally very stable. Due to this stability PAH are abundant molecules in the combustion zone [17]. Nanoparticles consisting mainly of carbon and PAH are always formed together in combustion processes, and it is believed by some that PAH are the molecular precursors of soot. However, it is more likely that PAH are a side branch in the process that forms the carbonaceous nanoparticles [18]. At the high temperature in the combustion zone, PAH are in the gas phase. Yet when the exhaust gases cool down to ambient temperature, the heavy PAH with 4 and more rings adsorb at the surface of the carbonaceous particles. This is where they can be detected with great efficiency by photoelectric charging (PC) of the particles. The particles with the carbonaceous skeleton are the carriers by which the particle bound PAH (PPAH) are transported deep into the respiratory system. when the highly water insoluble PAH come into contact with living human tissue, the cells try to get rid of the PAH by making them water soluble. Unfortunately, this oxidation process creates the very strong, ultimate carcinogen which irreversibly binds to the DNA. A causal link between lung cancer in humans and the five-ring PAH Benzo(a)pyrene has been established [5].

The detection limit of PPAH with PC is about $1 \text{ ng}/\text{m}^3$ at a time resolution of 1 sec [8]. This is a very small amount of material, and the question of what this means for human

health arises. As the impact on human health from smoking cigarettes is known to many of us from personal experience we propose to use, instead of nanograms/m³, the daily cigarette exposure equivalent [18]. We assume that a standard cigarette smoker inhales a total mass of 200 ng of PPAH with each cigarette. The average minimum volume of air needed by humans in 24 h is $A = 11 \text{ m}^3$. Hence the PPAH-concentration which is equivalent to smoking one cigarette per day is $a = M/A = 18.2 \text{ ng/m}^3$. As an example, a taxi ride from CDC-airport to the center of Paris means smoking $(659/200)11/24 \cdot 1.5 = 2.3$ standard cigarettes, compare Fig. 4.

Naturally, we do not content that the risk from Diesel fumes is the same as the one from cigarette smoke. The cigarette equivalent is only meant to provide an order of magnitude estimate for the individual health risk imposed by suspended nanoparticles from combustion [18]. What this precisely means is that the PPAH allow one to intercompare the nanoparticles from different combustion sources.

We have done some preliminary measurements in Mexico City. The PPAH concentrations on the motorways were very similar or even below the ones found in Paris, yet larger particles were detected by light scattering (LS) in much greater densities. Of course, these large visible particles give Mexico City the bad reputation with respect to particulate air pollution. On the other hand side, one has to know that the

nanoparticles attach themselves to the surface of the large particles, hence the microparticles act as scavengers of the nanoparticles. This means that the deposition in the lung is reduced. It is certainly not enough to remove the microparticles in electrofilters as has been done in the industrialized countries. Care must be taken to reduce the nanoparticles as well. It has been demonstrated that this is possible in particle traps at the exhaust of Diesel engines [19]. If a fuel additive such as $\text{Fe}(\text{C}_5\text{H}_5)_2$ is used, the particles burn in the trap at exhaust temperature, hence the particle trap has a reasonably long lifetime. The legislator must know how to act and make such particle traps mandatory on Diesel vehicles. Research with nanoparticles is both important and rewarding, even for fundamental research. Very small particles in gas suspension may have unique properties that still need to be discovered or verified.

6. Acknowledgments

We thank Prof. Araki and Prof. Sakai for the hospitality while the data in Tokyo were taken. We also thank "Sciences et Avenir" for making the measurements in Paris possible. Furthermore, we are indebted to Alejandro Keller who took the first measurements in Mexico City; and, last but not least, to Leo Scherrer for the fine PC- and DC-instruments he has built for us.

1. F. Hofer, P. Warbichler, and W. Grogger, *Spektrum der Wissenschaft* (Oct. 1998) 48.
2. J.J. Godleski *et al.*, *Proc. 2nd Coll. on Particulate Air Pollution and Human Health* **4** (1996) 136.
3. P. Leuenberger *et al.*, and Spapalida Team, "Swiss Study on Air Pollution and Lung Diseases in Adults", *Final Report to the Swiss Nat. Res. Foundation*, Lausanne/Basel 19955.
4. E. Weingartner, H. Burtscher, and U. Baltensperger, *Atmospheric Environment* **31** (1997) 2311.
5. M.F. Denissenko, A. Pao, M.S. Tang, and G.P. Pfeiffer, *Science* **274** (1996) 430.
6. A. Schmidt-Ott, P. Schurtenberger, and H.C. Siegmann, *Phys. Rev. Lett.* **45** (1980) 1284.
7. M. Kasper *et al.*, *J. of El. Spectroscopy and Related Phenomena* (1998), (in press).
8. H. Burtscher and H.C. Siegmann, *Combust. Sci. and Tech.* **101** (1994) 327.
9. M. Kasper, K. Siegmann, *Combust. Sci. and Tech.* (1999) (submitted); M. Kasper *et al.*, *J. Aerosol Sci.* **30** (1999) (in press).
10. Ch. Hüglin, J. Paul, L. Scherrer, and K. Siegmann, *J. Phys. Chem.* **101** (1997) 9335.
11. M. Fierz *et al.*, *J. Apply Phys. B*, (March 1999) (in press).
12. J. Paul, A. Dörzbach, and K. Siegmann, *Phys. Rev. Lett.* **79** (1997) 2947.
13. G. Skillas *et al.*, "Determination of air exchange rates of rooms and deposition factors for fine particles", *Environm. Sci. & Technology*, (submitted).
14. B. Schleicher, H. Burtscher, and H.C. Siegmann, *Appl. Phys. Lett.* **63** (1993) 1191.
15. M. Ammann *et al.*, *Geophys. Res. Lett.* **19** (1992) 1387.
16. E. Weingartner *et al.*, *Atmospheric Environment* **31** (1997) 451.
17. K. Siegmann, H. Hepp, and K. Sattler, *Combust. Sci. and Tech.* **109** (1995) 165.
18. K. Siegmann and H.C. Siegmann, in: *Current Problems in Condensed Matter*, edited by J.L. Moran-Lopez, (Plenum, New York, 1998).
19. A. Mayer *et al.*, *SAE International* **980539** (1998) 127.